



Surface acoustic wave characteristics of AlN thin films grown on a polycrystalline 3C-SiC buffer layer

Si-Hong Hoang, Gwi-Yang Chung *

School of Electrical Engineering, University of Ulsan, San 29, Mugeodong, Namgu, Ulsan 680-749, Republic of Korea

ARTICLE INFO

Article history:

Received 8 October 2008
Received in revised form 16 January 2009
Accepted 20 February 2009
Available online 6 March 2009

Keywords:

AlN thin film
Polycrystalline 3C-SiC
Two-port SAW resonator
SAW properties

ABSTRACT

In this study, AlN thin films were deposited on a polycrystalline (poly) 3C-SiC buffer layer for surface acoustic wave (SAW) applications using a pulsed reactive magnetron sputtering system. AFM, XRD and FT-IR were used to analyze structural properties and the morphology of the AlN/3C-SiC thin film. Suitability of the film in SAW applications was investigated by comparing the SAW characteristics of an interdigital transducer (IDT)/AlN/3C-SiC structure with the IDT/AlN/Si structure at 160 MHz in the temperature range 30–150 °C. These experimental results showed that AlN films on the poly (111) preferred 3C-SiC have dominant *c*-axis orientation. Furthermore, the film showed improved temperature stability for the SAW device, TCF = −18 ppm/°C. The change in resonance frequency according to temperature was nearly linear. The insertion loss decrease was about 0.033 dB/°C. However, some defects existed in the film, which caused a slight reduction in SAW velocity.

© 2009 Elsevier B.V. All rights reserved.

1. Introduction

AlN has been widely used in thin film form for SAW applications because of its attractive material properties including: high electrical resistance, acoustic velocity, temperature and chemical stability and piezoelectric properties. Currently, AlN films grown on different substrates revealed many advantages such as high SAW velocity in AlN/diamond, AlN/sapphire, AlN/4H-SiC and AlN/6H-SiC embodiments [1–4], and low temperature coefficient of frequency (TCF) in AlN/Sapphire [2], AlN/diamond [5] and AlN/6H-SiC [6] systems. Unfortunately, these structures still have some disadvantages. As-deposited poly diamond films exhibit poor surface roughness and high hardness. These disadvantages are improved by using a diamond (backside)/Si structure, or nanocrystalline diamond [5,7], which is based on a complex process and therefore is relatively expensive. SiC wafers (4H- and 6H-bulk) fabricated by a sublimation method are commercially available, but these substrates have small areas and are very costly because it is difficult to obtain large area substrates by sublimation due to the high temperature (2000 °C) required. Moreover, these materials are hard to integrate into the silicon device fabrication process and are not compatible with other electronic elements. So, the main drawbacks of these substrates are that they are expensive and difficult to integrate into conventional Si manufacturing technologies. Si substrates, on the other hand, are low cost but the difference in coefficient of thermal expansion (CTE) (17%) and

the lattice mismatch (19%) between AlN and Si are large, which is a disadvantage for their SAW properties at high temperatures.

Recently, SiC-MEMS researchers have become interested in cubic 3C-SiC that can be grown on large Si wafers at relatively low cost. 3C-SiC is classified into single and polycrystalline types by its crystal structure. In comparison with poly 3C-SiC films, single 3C-SiC films require high growth temperatures, which cause problems such as a large residual stress, cracks, lattice mismatching (20%), and different CTE (8%) at the Si/single-SiC interface. However, poly 3C-SiC grown on an insulating material like SiO₂ can reduce these problems because the growth temperature can be lower than that of single crystalline on other substrates [8]. Furthermore, The SiC's CTE is closely matched that of AlN, and the lattice mismatch is less than 1%. Therefore, both materials have been used in applications in high temperature packaging [9], and AlN thin films have been used as buffer layers for 3C-SiC grown on Si substrate [10].

Based on the discussion above, poly 3C-SiC is an ideal candidate for a buffer layer of poly AlN films grown on SiO₂/Si substrate for SAW applications with variable temperature, which is the topic of this work. A pulsed magnetron reactive sputtering method was used to deposit AlN on 3C-SiC buffer layer. The structural properties of AlN/SiC were investigated by atomic force microscopy (AFM), X-ray diffraction (XRD), and Fourier transform infrared spectroscopy (FT-IR). The sample poly AlN(0002) grown on Si(100) substrate was used. We fabricated an IDT/AlN/3C-SiC structure and an IDT/AlN/Si structure with the same wavelength (λ) and thickness (h), and investigated their SAW properties over the temperature range 30–150 °C.

* Corresponding author. Tel.: +82 52 259 1248; fax: +82 52 259 1686.
E-mail address: gschung@ulsan.ac.kr (G.-S. Chung).

2. Experimental

The (100) oriented Si wafer was cut into a rectangular shape of $4 \times 6 \text{ cm}^2$. After an 800 nm SiO_2 layer was grown on the Si wafer using a wet thermal oxidization process, poly 3C-SiC thin film (used as a buffer layer) was deposited on the oxidized Si(100) substrate by atmospheric pressure chemical vapor deposition (APCVD) using Ar + H_2 mixtures as a carrier gas and hexamethyldisilane (HMDS: $(\text{CH}_3)_6\text{Si}_2$) as a precursor. Poly 3C-SiC thin film with 0.5 μm thickness was grown at a deposition temperature of 1100 °C [8]. AlN thin films with 2 μm thickness were deposited on the poly 3C-SiC/ SiO_2 /Si substrates and the Si wafers in the same deposition condition by using a 40 kHz pulsed magnetron reactive sputtering system. The distance between the aluminum (Al) target (99.999% purity) and the substrate was 8 cm. After the sputtering chamber was evacuated to a base pressure of 5×10^{-7} Torr, AlN films were deposited at a deposition pressure of 3.5×10^{-3} Torr with gas flow ratio (Ar: N_2) of 10:1. Deposition rate was 800–850 Å/min. During the deposition, the applied power density was 12.5 W/cm^2 and substrate was at room temperature. The phases of the films were determined by a high resolution triple axis X-ray diffractometer (HRXRD: Philips X'Pert Pro-MRD) in the Bragg-Brentano geometry, using Cu-K α radiation. XRD diffraction angles (2θ) were in range from 20° to 80°. In order to identify the chemical composition and structure of AlN/SiC films grown on oxidized Si substrate, the infrared absorption spectrum was measured at room temperature with the FTS-2000 Scimitar spectrometer. The AFM micrograph to observe the surface morphology was taken by a Digital Instrument SPA-400 microscope.

Two-port SAW resonators were fabricated by the conventional photolithography technology and wet etching. Inter-digital transducers (IDT) and reflectors (Aluminum) is 100 nm thick. IDTs of 50 finger pairs having an electrode period (d) of 8 μm were used. The number of grating finger was 50 per reflector. The grating width and a gap of reflector was 8 μm , the aperture was $W = 60 \lambda$, and the wavelength ($\lambda = 4d$) was 32 μm . The length from center to center was 2240 μm , and the spacing between the IDT and the reflector was 170 μm . Transmission characteristics of the two-port SAW resonators were measured using an Agilent 8802A Network Analyzer in the temperature range of 30–150 °C.

3. Results and discussion

Fig. 1 shows the XRD pattern of a poly 3C-SiC film grown on oxidized Si(100) substrate. Among the two peaks, the stronger one appeared at $2\theta = 35.54^\circ$, which is characteristic of the SiC(111) plane. The other peak presented at $2\theta = 60.24^\circ$, characteristic of the

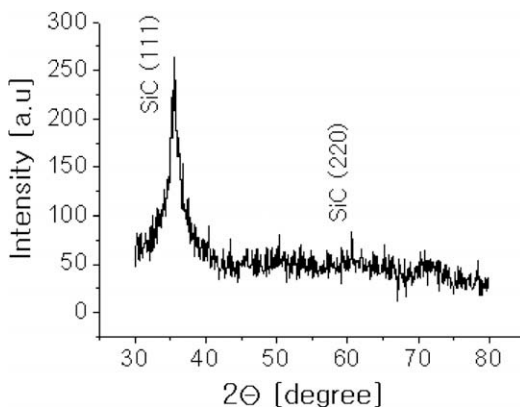


Fig. 1. XRD spectrum of poly 3C-SiC thin films deposited on the oxidized Si(100) substrate.

the SiC(220) plane. From XRD results, then, it is clear that poly 3C-SiC films grown on the oxidized Si substrate had a (111) preferred orientation.

In Fig. 2, the XRD spectrum of the AlN/SiC structure shows that the peak with the highest intensity is observed at $2\theta = 36.05^\circ$, indicating the (0002) oriented plane. The full width of half maximum (FWHM) of the (0002) AlN rocking curves was approximately 1.3°. This result suggests that the crystalline AlN of films grown on the poly 3C-SiC buffer layer were oriented along the c -axis normal to the substrate. However, other non-(0002) peaks appeared at $2\theta = 49.85$ and 66.08° indicating $(10\bar{1}2)$ and $(10\bar{1}3)$ planes, which are related with some defects that degrade the piezoelectric properties of the thin films [11]. The existence of these defects was confirmed by FT-IR analysis. The effect of these defects was investigated by measuring the SAW velocity of the film. On the other hand, the peak indicating the (111) plane of 3C-SiC film was not seen in Fig. 2. The reason for this is that the difference between the 3C-SiC(111) plane peak and the AlN(0002) plane peak is only $2\theta \times 0.6^\circ$ according to the data in Joint Committee on Powder Diffraction Standards (JCPDS). The existence of SiC layer was verified in the FT-IR absorption spectra.

Four kinds of stretching vibrations are observed in Fig. 3. The peak at around 810.1 cm^{-1} indicates that SiC exists in the films. The SiO_2 peak appeared at approximately 1095.6 cm^{-1} , while peaks at 613.4 and 671.2 cm^{-1} correspond to the Al(TO) and

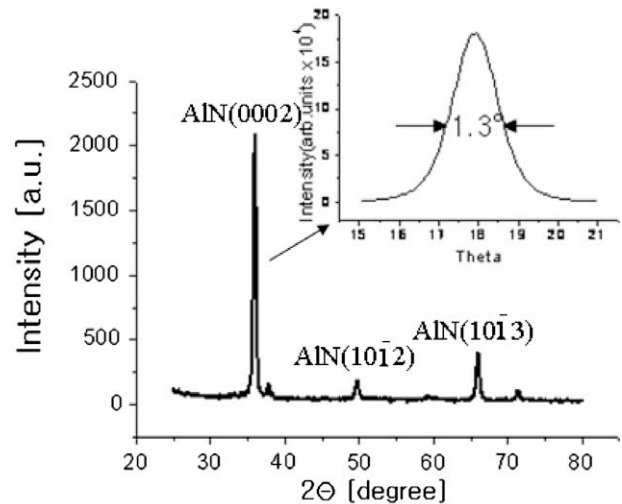


Fig. 2. XRD spectra of AlN/SiC structure and the rocking curve (inset) around the (0002) reflection.

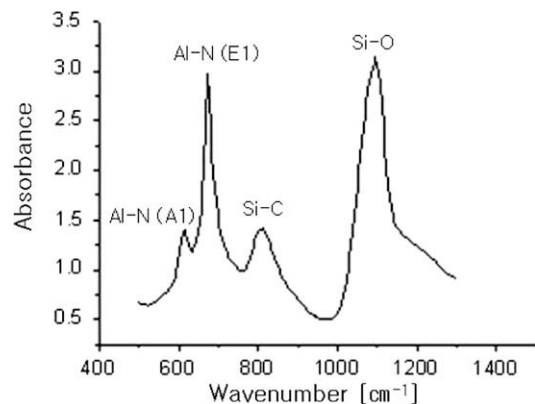


Fig. 3. FT-IR absorption spectra of the AlN/SiC structure.

E1(TO) vibrational modes of wurtzite AlN, respectively. The A1(TO) mode of AlN is related to the existence of grains of mixed orientations in the films while the ratio of integrated areas of A1(TO) vibrational mode over the E1(TO) mode are related to the (0002) preferred orientation of the films [12]. The energy of E1(TO) and A1(TO) peaks were intense and weak, respectively, which confirm the dominant of the (0002) orientation.

Generally, a (111) plane in FCC (face-centered cubic) structure is well matched with a (0002) plane in a hexagonal structure. Lattice mismatch between AlN films and 3C-SiC buffer layer was approximately 1%. The as-grown AlN thin films on 3C-SiC buffer layer had a low root mean square (RMS) roughness of about 9.3 nm, as shown in Fig. 4. Thus, although weak (10 $\bar{1}$ 2) and (10 $\bar{1}$ 3) planes were still existent in the film, clear (0002) orientation of poly AlN films on a poly 3C-SiC buffer layer with (111) orientation were achieved by using pulsed reactive magnetron sputtering, which is promising for using in SAW applications.

Fig. 5 shows the frequency responses of two-port SAW resonators fabricated on AlN/3C-SiC/SiO₂/Si and AlN/Si samples at room temperature. The SAW velocity of the AlN/3C-SiC SAW resonator was 5020.8 m/s at $h/\lambda = 0.0625$ ($h = 2 \mu\text{m}$, $\lambda = 32 \mu\text{m}$), with a corre-

sponding resonance frequency of 156.9 MHz as shown Fig. 5a. This SAW velocity was 153.6 m/s lower than the SAW velocity (5174.4 m/s) of an AlN/Si sample (Fig. 5b) with the same h and λ . These results can be caused by the appearance of some non-(0002) peaks in the XRD spectrum of the AlN/SiC structure, which was explained above. Nevertheless, with $\lambda = 32 \mu\text{m}$, the SAW velocity of the AlN/3C-SiC SAW resonator is high and can be made higher by reducing the resolution of the IDTs and reflector gratings by e-beam lithography [3].

Fig. 6 shows the change in insertion loss of SAW resonators in the temperature range of 30–150 °C. In the range of 30–80 °C, delta IL (ΔIL) changes are similar in both an IDT/AlN/3C-SiC and IDT/AlN/Si structures. The change in ΔIL for AlN/Si sample is irregular when compared with that of AlN/3C-SiC in range of 80–150 °C. In addition, the insertion loss of the IDT/AlN/3C-SiC structure was -21.92 dB with 9.3 nm RMS roughness at room temperature; the change in insertion loss is approximately linear and decreases by 0.033 dB/°C in the temperature range from 30 to 150 °C. This insertion loss is significant when the temperature increase is high.

Fig. 7 shows the fractional change in the resonance frequency ($(f - f_0)/f_0$) of SAW resonators as a function of temperature in the

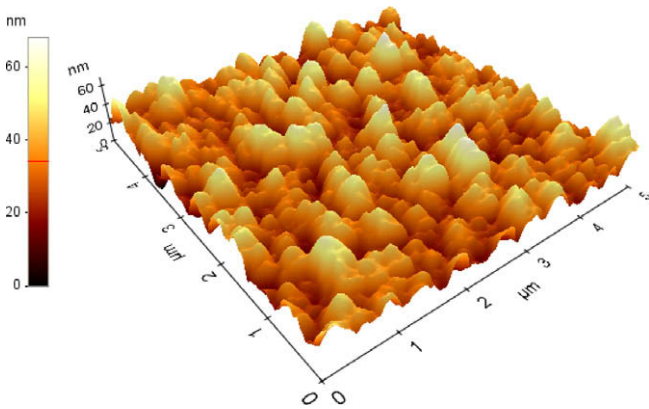


Fig. 4. AFM image of the AlN/SiC structure.

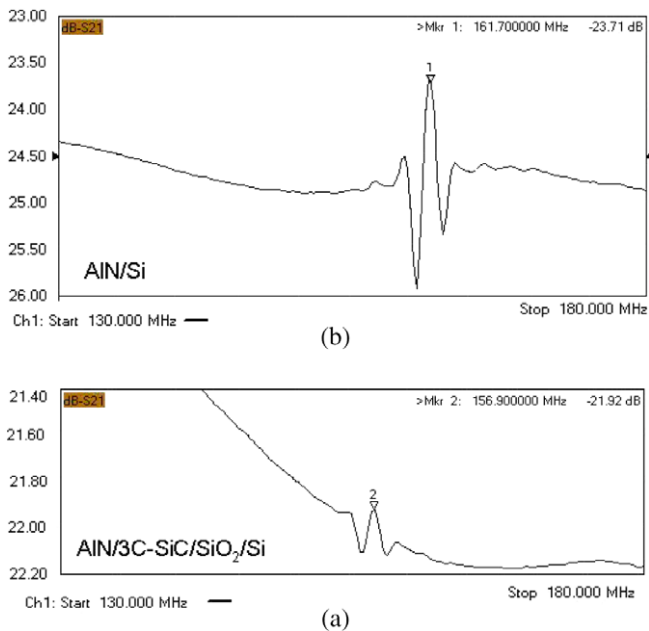


Fig. 5. Frequency response of two-port SAW resonators: (a) AlN on 3C-SiC/SiO₂/Si substrate; (b) AlN on Si substrate.

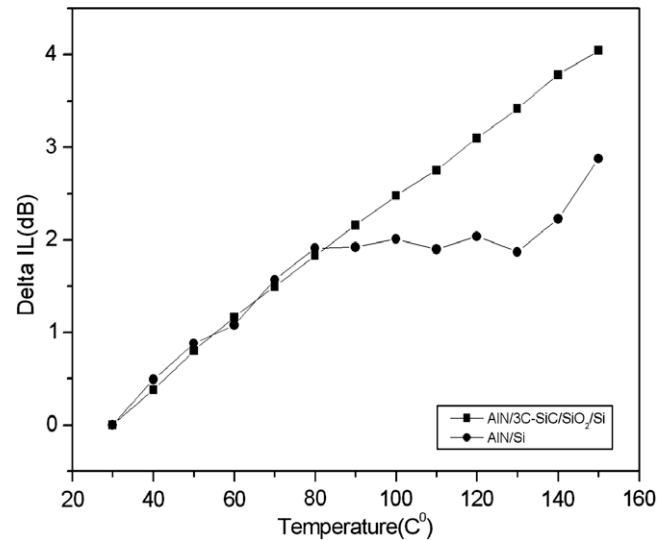


Fig. 6. The change of insertion loss of two-port SAW resonators using AlN/3C-SiC and AlN/Si structures as a function of temperature.

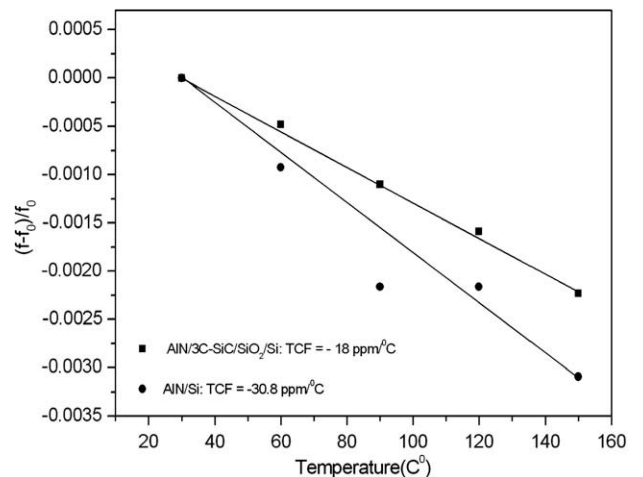


Fig. 7. Temperature dependence of the center frequency of two-port SAW resonators using AlN/3C-SiC and AlN/Si structures.

range of 30–150 °C, where f_0 was selected as the frequency at 30 °C (room temperature). The TCF was calculated from the following equation: $TCF = (df/dT) \times 1/f_0$. The TCF of AlN/3C-SiC sample was about $-18 \text{ ppm}/^\circ\text{C}$ with $h/\lambda = 0.0625$. This value is better than the value of $-30.8 \text{ ppm}/^\circ\text{C}$ obtained for AlN/Si as in Fig. 7, which is comparable with that of materials often used in SAW devices: $13.4 \text{ ppm}/^\circ\text{C}$ in AlN/diamond [5] and $-19 \text{ ppm}/^\circ\text{C}$ in bulk AlN single crystal [13] and $-28.21 \text{ ppm}/^\circ\text{C}$ in AlN/Y-128 LiNbO₃ [14]. Our $-18 \text{ ppm}/^\circ\text{C}$ result is smaller than the $-20.5 \text{ ppm}/^\circ\text{C}$ for AlN grown on 6H-SiC(0001) substrate [6]. This difference in TCF can be caused by the restricted temperature [6] or SiO₂ buffer layer. Moreover, the decrease in resonance frequency according to the increase in temperature of the IDT/AlN/3C-SiC structure is nearly linear.

4. Conclusions

Poly AlN thin films were deposited on a poly 3C-SiC buffer layer by pulsed reactive magnetron sputtering. The films had a smooth surface with a RMS of 9.3 nm. The XRD spectra of 3C-SiC films showed a (111) preferred orientation. From the results of both XRD and FT-IR analysis, AlN thin films grown on poly 3C-SiC buffer layer still exists some undesired defects such as (10 $\bar{1}$ 2) and (10 $\bar{1}$ 3) planes, which caused a light decrease in SAW velocity. However, using poly 3C-SiC as the buffer layer for AlN grown on SiO₂/Si substrate brings satisfactory results for SAW properties over the temperature range from 30 to 150 °C. The results indicate that the change in resonance frequency is nearly linear with changes in temperature, and that of the TCF of device is small (about 18 ppm/°C). The decrease of the insertion loss is about 0.033 dB/°C. The temperature-basis frequency response of the two-port SAW resonator of AlN films deposited on 3C-SiC buffer layers are enhanced significantly when compared with the resonator of AlN

film grown on Si substrate. Therefore, the poly AlN grown on the poly 3C-SiC buffer layer can be used for SAW applications with various temperatures, which is the basis for study of SAW applications in harsh temperature environments with low cost.

Acknowledgement

This research was financially supported by the Grant no. B0009720 from the Regional Technology Innovation Program of the Ministry of Knowledge Economy.

References

- [1] P. Kirsch, M.B. Assouar, O. Elmazria, V. Mortet, P. Alnot, *Appl. Phys. Lett.* **88** (2006) 223504-1.
- [2] K. Uehara, Y. Aota, T. Shibata, S. Kameda, H. Nakase, Y. Isota, K. Tsubouchi, *Jpn. J. Appl. Phys.* **44** (2005) 4512.
- [3] Y. Takagaki, P.V. Santos, E. Wiebicke, O. Brandt, H.-P. Schonherr, K.H. Ploog, *Appl. Phys. Lett.* **81** (2002) 2538.
- [4] K. Uehara, C.-M. Yang, T. Furusho, S.-K. Kim, S. Kameda, H. Nakase, S. Nishino, K. Tsubouchi, *IEEE Ultrason. Symp.* **1** (2003) 905.
- [5] O. Elmazria, V. Mortet, M. El Hakiki, M. Nesladek, P. Alnot, *IEEE Trans. Ultrason. Ferr.* **50** (2003) 710.
- [6] R. Cuervo, J. Pedrós, A. Navarro, A.F. Braña, J.L. Pau, E. Muñoz, F. Calle, *J. Mater. Sci. Mater. Electron.* **19** (2008) 189.
- [7] F. Bénédic, M.B. Assouar, F. Mohasseb, O. Elmazria, P. Alnot, A. Gicquel, *Diam. Relat. Mater.* **13** (2004) 347.
- [8] G.S. Chung, K.S. Kim, *J. Korean Phys. Soc.* **51** (4) (2007) 1389.
- [9] Z. Lin, R.J. Yoon, *Proc. Int. Symp.* (2005) 156.
- [10] G.S. Chung, K.S. Kim, *Electron. Lett.* **43** (2007) 832.
- [11] A. Sanz-Hervás, M. Clement, E. Iborra, L. Vergara, J. Olivares, J. Sangrador, *Appl. Phys. Lett.* **88** (2006) 161915-1.
- [12] A. Sanz-Hervás, E. Iborra, M. Clement, J. Sangrador, M. Aguilar, *Diam. Relat. Mater.* **12** (2003) 1186.
- [13] G. Bu, D. Ciplys, M. Shur, L.J. Schowalter, S. Schujman, R. Gaska, *Electron. Lett.* **39** (2003) 755.
- [14] S. Wu, Y.-C. Chen, Y.S. Chang, *Jpn. J. Appl. Phys.* **41** (2002) 4605.